4th Biannual Post Graduate Conference
18th-20th November 2015, Seri Iskandar, Perak

# Simulation and Development of Performance Correlations of 3-D Turning Diffuser via ACFD

Normayati Nordin
Faculty of Mechanical and Manufacturing Engineering
Universiti Tun Hussein Onn Malaysia
Batu Pahat, Malaysia
mayati@uthm.edu.my

Zainal Ambri Abdul Karim
Department of Mechanical Engineering
Universiti Teknologi Petronas
Tronoh, Malaysia
ambri@petronas.com.my

Safiah Othman (Former lecturer)
Faculty of Mechanical and Manufacturing Engineering
Universiti Tun Hussein Onn Malaysia
Batu Pahat, Malaysia
safiah@uthm.edu.my

Vijay R. Raghavan
OYL Research & Development Centre
OYL Research & Development Sdn Bhd
Sungai Buloh, Malaysia
vijay@oyl.com.my

***Abstract*— This paper aims to intensively simulate the performances of 3-D turning diffuser by varying geometrical and operating parameters and to develop the performance correlation by means of Asymptotic Computational Fluid Dynamic (ACFD) technique. The performances of turning diffusers were measured primarily by outlet pressure recovery coefficient, $C_p$ and flow uniformity index, $\sigma_{out}$. The geometrical and operating parameters namely inflow Reynolds number ($Re_{in}$ = 5.786 x $10^4$ – 1.775 x $10^5$), inlet throat width ratio ($L_{in}/W_1$ = 1.5 - 25.0) and outlet-inlet configurations ($W_2/W_1$ = 1.067 – 2.667 and $X_2/X_1$ = 1.118 – 2.778) were varied. The performance correlations as a function of geometrical and operating parameters, i.e. $C_p = f(L_{in}/W_1, W_2/W_1, X_2/X_1, Re_{in})$ and $\sigma_{out} = f(L_{in}/W_1, W_2/W_1, X_2/X_1, Re_{in})$ are successfully developed via ACFD with deviation to the experiment approximately of 7%.**

***Keywords*— ACFD; CFD; turning diffuser**

## I. INTRODUCTION

Study of the geometry effect on diffuser performance has been of fundamental interest to researchers in the area of fluid mechanics since decades and it continues to grow [1-8]. The performance of diffuser is primarily evaluated by means of:

(i) Outlet pressure recovery coefficient ($C_p$)

$$C_p = \frac{2(P_{out} - P_{in})}{\rho V_{in}^2} \quad (1)$$

where,
$P_{out}$= outlet static pressure (Pa)
$P_{in}$= inlet static pressure (Pa)
$\rho$ = flow density (kg/m$^3$)
$V_{in}$ = inlet air velocity (m/s)

(ii) Flow uniformity index ($\sigma_{out}$)

$$\sigma_{out} = \sqrt{\frac{1}{N-1}\sum_{i=1}^{N}(V_i - V_{out})^2} \quad (2)$$

where,
$N$= number of measurement points
$V_i$= local outlet air velocity (m/s)
$V_{out}$= mean outlet air velocity (m/s)

The value of $C_p$ indicates how much kinetic energy is successfully converted to pressure energy. The main problem in achieving high pressure recovery is flow separation, which results in non-uniform flow distribution. The $\sigma_{out}$ is used to measure the dispersion of local velocity from the mean velocity. It is strongly dependent on the distribution of core flow and the presences of secondary flow. The flow is considered uniform with the presences of secondary flow of less than 10%.

In the current work, the performance of 3-D turning diffuser with 90$^o$ angle of turn ($\Delta\phi$) as shown in Fig. 1 is intensively simulated by varying geometrical and operating parameters namely inflow Reynolds number ($Re_{in}$= 5.786 x $10^4$ – 1.775 x $10^5$), inlet throat width ratio ($L_{in}/W_1$= 1.5 - 25.0) and outlet-inlet configurations ($W_2/W_1$= 1.067 – 2.667 and $X_2/X_1$ = 1.118 – 2.778).

Asymptotic Computational Fluid Dynamic (ACFD) is a relatively new analytical technique established by Herwig et al. that applies Taylor Series expansion to produce correlations between all the relevant non-dimensional variables of the problem analysed by CFD [9-12]. This technique requires less number of solutions $n$ + 1 than the usual-used linear regression and curve fitting techniques, $4^n$

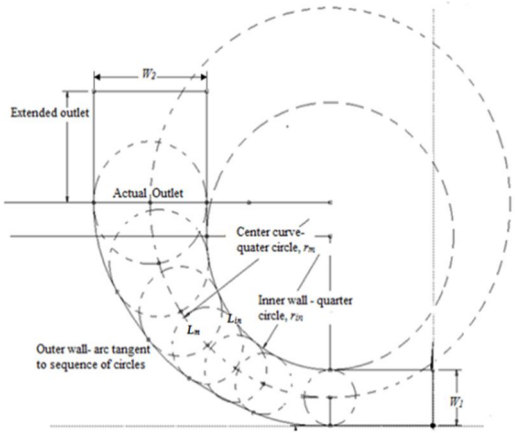


(a)

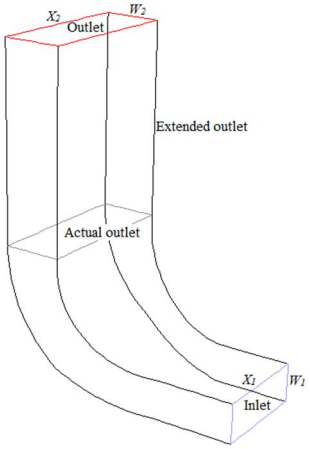


(b)

Fig. 1 A 90° 3-D turning diffuser (a) longitudinal section (b) isometric view

number of solutions to develop correlations from the CFD simulations, where *n* represents non-dimensional variables.

The performance correlations as a function of geometrical and operating parameters of 3-D turning diffuser are developed in the current work by means of ACFD, i.e. $C_p = f\ (L_{in}/W_1,\ W_2/W_1,\ X_2/X_1,\ Re_{in})$ and $\sigma_{out} = f\ (L_{in}/W_1,\ W_2/W_1,\ X_2/X_1,\ Re_{in})$. These correlations minimise time and effort needed by other researchers to evaluate the performances of 3-D turning diffuser without necessarily of their own simulating the system.

## II. CFD METHODOLOGY

The $C_p$ and $\sigma_{out}$ were obtained from the CFD simulations by varying each geometrical and operating parameter within the specified range to five set of solutions. The reference case was prescribed at $Re_{in\ ref} = 6.382 \times 10^4$, $W_2/W_{1ref} = 1.44$, $X_2/X_{1ref} = 1.50$, $L_{in}/W_{1ref} = 3.99$. Other performance indicators such as loss coefficient ($K$), dispersion of core flow ($\sigma_y$), separation point ($S$) and secondary flow index ($S_{out}$) were considered to comprehensively discuss the results.

The following three-dimensional steady-state Reynolds Averaged Navier Stokes (RANS) equations were numerically solved:

Continuity equation:

$$\frac{\partial u}{\partial x}+\frac{\partial v}{\partial y}+\frac{\partial w}{\partial z}=0 \tag{3}$$

x- momentum equation:

$$u\frac{\partial u}{\partial x}+v\frac{\partial u}{\partial y}+w\frac{\partial u}{\partial z}=-\frac{1}{\rho}\frac{\partial P}{\partial x}+\nu\left[\frac{\partial^2 u}{\partial x^2}+\frac{\partial^2 u}{\partial y^2}+\frac{\partial^2 u}{\partial z^2}\right] +\frac{1}{\rho}\left[\frac{\partial(-\rho\overline{u'^2})}{\partial x}+\frac{\partial(-\rho\overline{u'v'})}{\partial y}+\frac{\partial(-\rho\overline{u'w'})}{\partial z}\right] \tag{4}$$

y- momentum equation:

$$u\frac{\partial v}{\partial x}+v\frac{\partial v}{\partial y}+w\frac{\partial v}{\partial z}=-\frac{1}{\rho}\frac{\partial P}{\partial y}+\nu\left[\frac{\partial^2 v}{\partial x^2}+\frac{\partial^2 v}{\partial y^2}+\frac{\partial^2 v}{\partial z^2}\right] +\frac{1}{\rho}\left[\frac{\partial(-\rho\overline{u'v'})}{\partial x}+\frac{\partial(-\rho\overline{v'^2})}{\partial y}+\frac{\partial(-\rho\overline{v'w'})}{\partial z}\right] \tag{5}$$

z- momentum equation:

$$u\frac{\partial w}{\partial x}+v\frac{\partial w}{\partial y}+w\frac{\partial w}{\partial z}=-\frac{1}{\rho}\frac{\partial P}{\partial z}+\nu\left[\frac{\partial^2 w}{\partial x^2}+\mu\frac{\partial^2 w}{\partial y^2}+ +\frac{1}{\rho}\left[\frac{\partial(-\rho\overline{u'w'})}{\partial x}-\frac{\partial(-\rho\overline{v'w'})}{\partial y}-\frac{\partial(-\rho\overline{w'^2})}{\partial z}\right] \tag{6}$$

The standard $k$-$\varepsilon$ turbulence model adopted enhanced wall treatment, $y^+ \approx$ 1.2 - 1.7 as successfully validated in the previous progress was applied [13-15]. Each governing equation was independently solved using a double precision pressure-based solver. A robust pressure-velocity coupling algorithm, SIMPLE which uses a combination of momentum and continuity equations to derive an equation for pressure (or pressure correction) was applied. To reduce numerical diffusion, the QUICK scheme was employed for the discretization of the momentum equations, the turbulent kinetic energy equation and the turbulent dissipation rate equation. A PRESTO discretization scheme was applied for the continuity equation and a default scheme, i.e. Green-

Gauss Cell-based, was employed for the solution of the gradient. The solutions were considered converged when the scaled residual of all simulated variables dropped to $10^{-6}$ and the conservation of overall mass balance through the domain boundary exceeded 99%.

## III. EFFECT OF VARYING GEOMETRICAL AND OPERATING PARAMETERS

Effects of varying geometrical and operating parameters ($Re_{in}$, $W_2/W_1$, $L_{in}/W_1$ and $X_2/X_1$) on the pressure recovery and flow uniformity of the 3-D turning diffusers are examined.

As depicted in Table 1, varying $Re_{in}$ from 5.786 x $10^4$ to 1.775 x $10^5$ provides significant influence on the $C_p$ and $\sigma_{out}$. The $C_p$ is affected by the existences of flow separation and vortices, whereas the $\sigma_{out}$ is resulted by the dispersion of core, $\sigma_y$ and secondary flows, $S_{out}$. Applying high $Re_{in}$ considerably influences the formation of vortices and onset flow separation of the 3-D turning diffuser as respectively shown in Fig. 2 and 3.

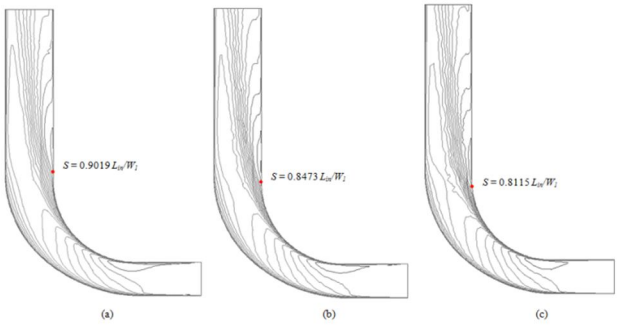


Fig. 2 Onset flow separation, $S$ at (a) $Re_{in}$ = 5.786 x $10^4$, (b) $Re_{in}$ = 1.027 x $10^5$ and (c) $Re_{in}$ = 1.775 x $10^5$

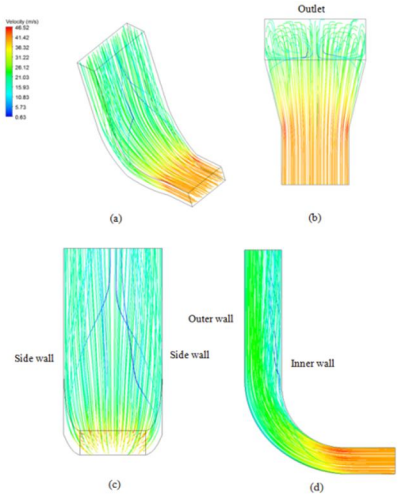


Fig. 3 Velocity streamlines at $Re_{in}$ = 1.775 x $10^5$ (a) isometric, (b) top, (c), front and (d) longitudinal views

Table 1 Effect of $Re_{in}$

| $Re_{in}$ | Recovery performance | | Flow performance | | |
|---|---|---|---|---|---|
| | $C_p$ | $K$ | $\sigma_{out}$ (m/s) | $\sigma_y$ (m/s) | $S_{out}$ |
| 5.786 x $10^4$ | 0.216 | 0.784 | 2.71 | 2.91 | 0.133 |
| 6.382 x $10^4$ | 0.221 | 0.779 | 2.96 | 3.19 | 0.134 |
| 1.027 x $10^5$ | 0.205 | 0.795 | 4.56 | 4.94 | 0.141 |
| 1.397 x $10^5$ | 0.224 | 0.776 | 5.91 | 6.49 | 0.142 |
| 1.775 x $10^5$ | 0.192 | 0.808 | 7.23 | 7.88 | 0.152 |

Table 2 Effect of $W_2/W_1$

| $W_2/W_1$ | Recovery performance | | Flow performance | | |
|---|---|---|---|---|---|
| | $C_p$ | $K$ | $\sigma_{out}$ (m/s) | $\sigma_y$ (m/s) | $S_{out}$ |
| 1.067 | 0.089 | 0.911 | 3.21 | 3.23 | 0.119 |
| 1.333 | 0.306 | 0.694 | 2.52 | 2.55 | 0.138 |
| 1.440 | 0.221 | 0.779 | 2.96 | 3.19 | 0.134 |
| 2.000 | 0.472 | 0.528 | 2.04 | 2.05 | 0.215 |
| 2.667 | 0.513 | 0.487 | 1.70 | 1.78 | 0.255 |

Table 3 Effect of $L_{in}/W_1$

| $L_{in}/W_1$ | Recovery performance | | Flow performance | | |
|---|---|---|---|---|---|
| | $C_p$ | $K$ | $\sigma_{out}$ (m/s) | $\sigma_y$ (m/s) | $S_{out}$ |
| 1.52 | -0.007 | 1.007 | 3.86 | 4.30 | 0.290 |
| 3.99 | 0.221 | 0.779 | 2.96 | 3.19 | 0.134 |
| 8.99 | 0.027 | 0.973 | 2.25 | 2.28 | 0.240 |
| 13.00 | -0.243 | 124.3 | 2.51 | 2.51 | 0.075 |
| 25.00 | -1.666 | 2.666 | 2.22 | 2.30 | 0.270 |

Table 4 Effect of $X_2/X_1$

| $X_2/X_1$ ($\theta$) | Recovery performance | | Flow performance | | |
|---|---|---|---|---|---|
| | $C_p$ | $K$ | $\sigma_{out}$ (m/s) | $\sigma_y$ (m/s) | $S_{out}$ |
| 1.118 (3.7°) | 0.080 | 0.920 | 3.38 | 3.43 | 0.111 |
| 1.389 (11.9°) | 0.192 | 0.808 | 3.02 | 3.18 | 0.125 |
| 1.500 (15.2°) | 0.221 | 0.779 | 2.96 | 3.19 | 0.134 |
| 2.090 (30.6°) | -0.049 | 1.049 | 3.30 | 3.65 | 0.369 |
| 2.778 (43.9°) | 0.373 | 0.627 | 1.49 | 1.40 | 0.308 |

Table 2 shows that the $C_p$ and $\sigma_{out}$ of the diffuser improve with the increase of $W_2/W_1$ to maximum due to high turbulence intensity blending up uniformly the flow and nominal existences of flow separation within the inner wall as respectively shown in Fig. 4 and 5.

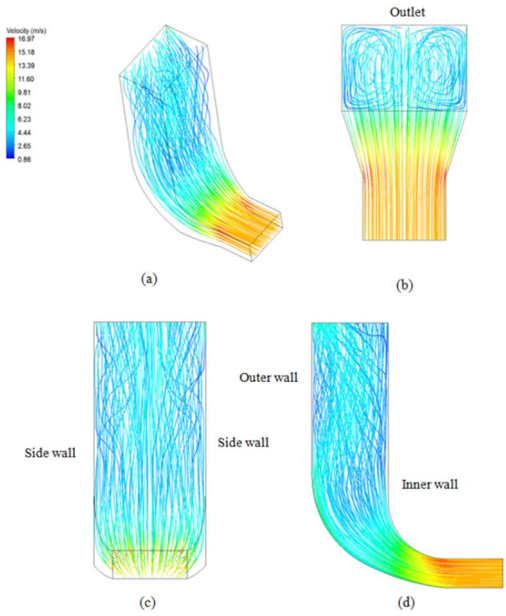


Fig. 4 Velocity streamlines at $W_2/W_1$ = 2.667 (a) isometric, (b) top, (c), front and (d) longitudinal views

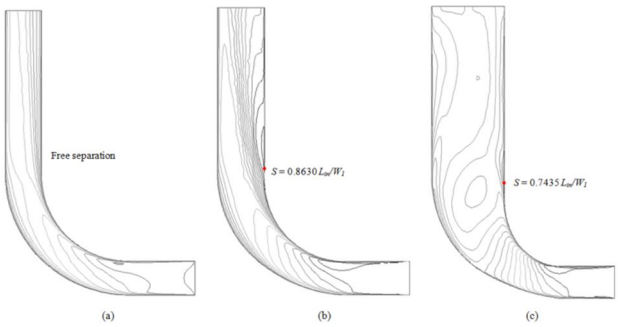


Fig. 5 Onset flow separation, $S$ at (a) $W_2/W_1$ = 1.067 (b) $W_2/W_1$ = 1.440 and (c) $W_2/W_1$ = 2.667

As depicted in Table 3, the best recovery of the 3-D turning diffuser, $C_p$ = 0.221 is attained by applying $L_{in}/W_1$ = 3.99. Nevertheless, elongating the diffuser $L_{in}/W_1 \geq 8.99$ may associate with skin friction loss that is found to affect severely the recovery regardless of zero separation (Fig. 6, 7 (b) and (c)). Elongating the 3-D turning diffuser to maximum, $L_{in}/W_1$ = 25.0 basically remedies the flow uniformity approximately of 43% from the worst, $\sigma_{out}$ = 3.86. This is attributed by less dispersion of core flow at relatively long $L_{in}/W_1$.

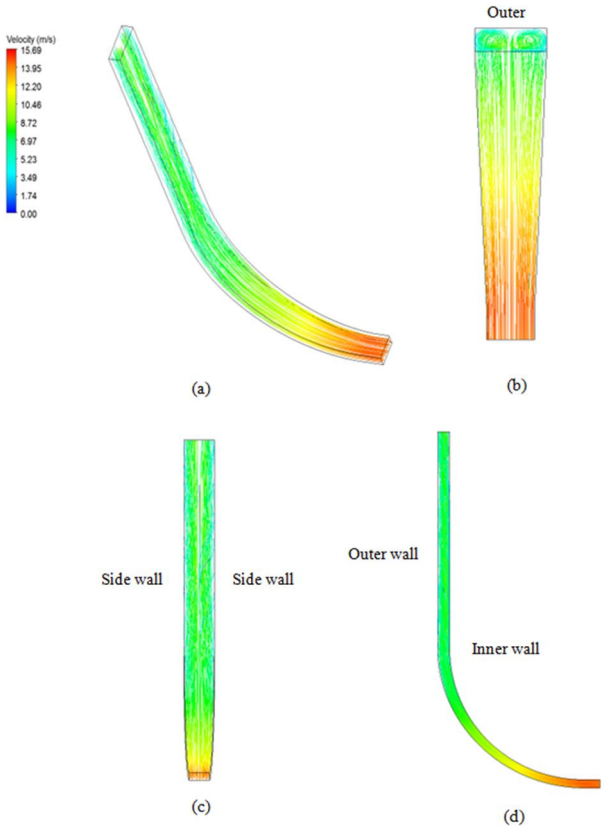


Fig. 6 Velocity streamlines at $L_{in}/W_1$ = 25.0 (a) isometric, (b) top, (c), front and (d) longitudinal views

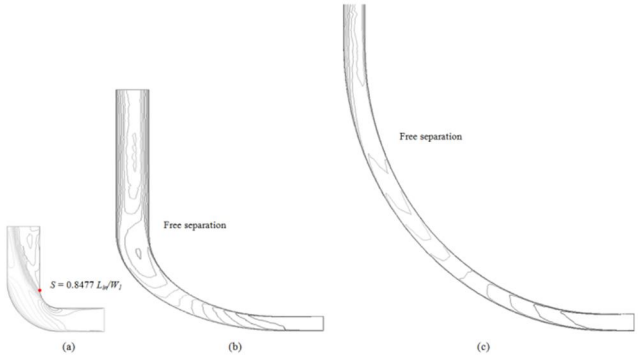


Fig. 7 Onset flow separation, $S$ at (a) $L_{in}/W_1$ = 1.52 (b) $L_{in}/W_1$ = 8.99 and (c) $L_{in}/W_1$ = 25.0

Table 4 shows that varying $X_2/X_1$ influences significantly the recovery and flow performances of the 3-D turning diffuser. Increasing the turbulent intensity could really impede the flow separation and lessen the growth of inner wall boundary layer hence provides promising pressure recovery and flow uniformity (see Figures 8 and 9).

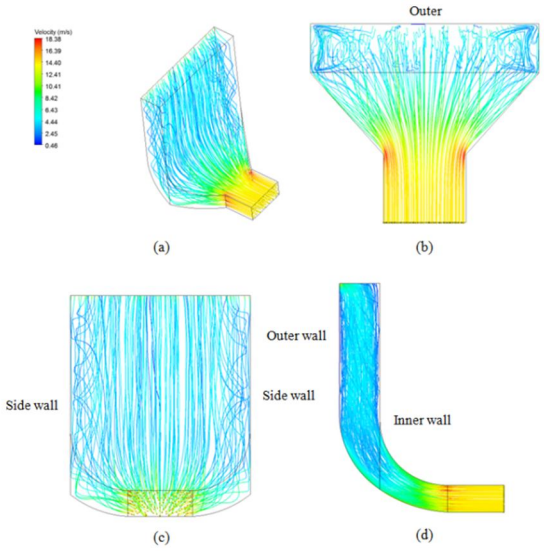


Fig. 8 Velocity streamlines at $X_2/X_1$ = 2.778 (a) isometric, (b) top, (c), front and (d) longitudinal views

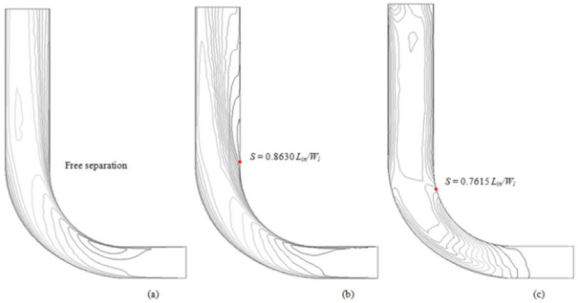


Fig. 9 Onset flow separation, $S$ at (a) $X_2/X_1$ = 1.118 (b) $X_2/X_1$ = 1.500 and (c) $X_2/X_1$ = 2.778

## IV. PERFORMANCE CORRELATIONS VIA ACFD

Applying Taylor Series expansion to find outlet pressure recovery ($C_p$) correlation:

$$C_{p\,3DTD\,acfd} = C_{p\,ref} + (\phi_1 - \phi_{1\,ref})\frac{\partial C_{p\,ref}}{\partial \phi_1} + (\phi_2 - \phi_{2\,ref})\frac{\partial C_{p\,ref}}{\partial \phi_2} + (\phi_3 - \phi_{3\,ref})\frac{\partial C_{p\,ref}}{\partial \phi_3} + (\phi_4 - \phi_{4\,ref})\frac{\partial C_{p\,ref}}{\partial \phi_4} \quad (2)$$

where,

$$\phi_1 = \left[\frac{Re_{in}}{Re_{in\,ref}}\right]^a, \phi_2 = \left[\frac{L_{in}/W_1}{L_{in}/W_{1_{ref}}}\right]^b, \phi_3 = \left[\frac{W_2/W_1}{W_2/W_{1_{ref}}}\right]^c,$$

$$\phi_4 = \left[\frac{X_2/X_1}{X_2/X_{1_{ref}}}\right]^d$$

$a = 2$, $b = 1$, $c = 3$, $d = 3$ are chosen so that all lines could fit in a graph as shown in Fig. 10 and intersect at a point that represents as $C_{p\,ref} = 0.230$

$\phi_{1\,ref} = \left[\frac{Re_{in\,ref}}{Re_{in\,ref}}\right]^a = 1.0$, thus $\phi_{2\,ref} = \phi_{3\,ref} = \phi_{4\,ref} = 1.0$

$\frac{\partial C_{p\,ref}}{\partial \phi_1} = -0.0028$, $\frac{\partial C_{p\,ref}}{\partial \phi_2} = -0.03056$, $\frac{\partial C_{p\,ref}}{\partial \phi_3} = 0.0592$, $\frac{\partial C_{p\,ref}}{\partial \phi_4} = 0.0306$ are slopes of the corresponding lines

Substituting all the constants in equation 2:

$$C_{p\,3DTD\,acfd} = 0.230 - \left(\left[\frac{Re_{in}}{Re_{in\,ref}}\right]^2 - 1\right)0.0028 - \left(\left[\frac{L_{in}/W_1}{L_{in}/W_{1ref}}\right]^1 - 1\right)0.03056 + \left(\left[\frac{W_2/W_1}{W_2/W_{1ref}}\right]^3 - 1\right)0.0592 + \left(\left[\frac{X_2/X_1}{X_2/X_{1_{ref}}}\right]^3 - 1\right)0.0306 \quad (3)$$

Applying Taylor Series expansion to find flow uniformity ($\sigma_{out}$) correlation:

$$\sigma_{out\,3DTD\,acfd} = \sigma_{out\,ref} + (\phi_1 - \phi_{1\,ref})\frac{\partial \sigma_{out\,ref}}{\partial \phi_1} + (\phi_2 - \phi_{2\,ref})\frac{\partial \sigma_{out\,ref}}{\partial \phi_2} + (\phi_3 - \phi_{3\,ref})\frac{\partial \sigma_{out\,ref}}{\partial \phi_{23}} + (\phi_4 - \phi_{4\,ref})\frac{\partial \sigma_{out\,ref}}{\partial \phi_4} \quad (4)$$

where,

$$\phi_1 = \left[\frac{Re_{in}}{Re_{in\,ref}}\right]^a, \phi_2 = \left[\frac{L_{in}/W_1}{L_{in}/W_{1_{ref}}}\right]^b, \phi_3 = \left[\frac{W_2/W_1}{W_2/W_{1_{ref}}}\right]^c,$$

$$\phi_4 = \left[\frac{X_2/X_1}{X_2/X_{1_{ref}}}\right]^d$$

$a = 2$, $b = 1$, $c = 3$, $d = 3$ are chosen so that all lines could fit in a graph as shown in Fig. 11 and intersect at a point that represents as $\sigma_{out\,ref} = 3.2$

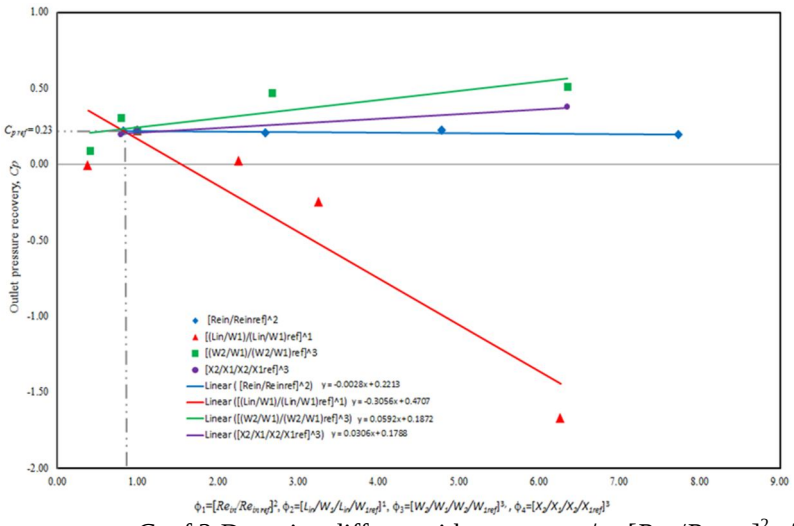


Fig. 10 Outlet pressure recovery, $C_p$ of 3-D turning diffuser with respect to $\phi_1 = [Re_{in}/Re_{in\,ref}]^2$, $\phi_2 = [L_{in}/W_1/L_{in}/W_{1ref}]^1$, $\phi_3 = [W_2/W_1/W_2/W_{1ref}]^3$ and $\phi_4 = [X_2/X_1/X_2/X_{1ref}]^3$

$\phi_{1\,ref} = \left[\frac{Re_{in\,ref}}{Re_{in\,ref}}\right]^a = 1.0$, thus $\phi_{2\,ref} = \phi_{3\,ref} = \phi_{4\,ref} = 1.0$

$\frac{\partial\,\sigma_{out\,ref}}{\partial\phi_1} = 0.6531$, $\frac{\partial\,\sigma_{out\,ref}}{\partial\phi_2} = -0.2202$, $\frac{\partial\,\sigma_{out\,ref}}{\partial\phi_3} =$ -0.2725, $\frac{\partial\,\sigma_{out\,ref}}{\partial\phi_4} = -0.2545$ are slopes of the corresponding lines

Substituting all the constants in equation 4:

$$\sigma_{out\,3DTD\,acfd} = 3.2 + \left(\left[\frac{Re_{in}}{Re_{in\,ref}}\right]^2 - 1\right)0.6531 - \left(\left[\frac{L_{in}/W_1}{L_{in}/W_{1ref}}\right]^1 - 1\right)0.2202 - \left(\left[\frac{\frac{W_2}{W_1}}{\frac{W_2}{W_{1ref}}}\right]^3 - 1\right)0.2725 - \left(\left[\frac{X_2/X_1}{X_2/X_{1ref}}\right]^3 - 1\right)0.2545 \quad (5)$$

$C_{p\ 3DTD\ acfd}$ and $\sigma_{out\ 3DTD\ acfd}$ obtained using developed correlations (3) and (5) are compared with the experimental results as respectively tabulated in Tables 5 and 6. Satisfied agreement between ACFD and experiment results with average deviation of 6.7 and 7.1% is respectively obtained. Hence, the developed correlations can be used as a guideline to preliminarily evaluate the performance of 3-D turning diffuser.

Table 5 Comparison of outlet pressure recovery coefficient ($C_p$) of 3-D turning diffuser obtained from ACFD correlation and experiment

| $\phi_{1,2,3}$ | No. | $C_{p\ 3DTD\ cfd}$ | $C_{p\ 3DTD\ acfd}$ | $C_{p\ 3DTD\ exp}$ | Deviation (%) |
|---|---|---|---|---|---|
| 0.822 | 1 | 0.216 | 0.230 | 0.210 | 9.8 |
| 1.000 | 2 | 0.221 | 0.230 | 0.217 | 6.0 |
| $\phi_1$ 2.590 | 3 | 0.205 | 0.226 | 0.203 | 11.1 |
| 4.792 | 4 | 0.224 | 0.219 | 0.219 | 0.2 |
| 7.735 | 5 | 0.192 | 0.211 | 0.194 | 8.8 |
| 0.381 | 6 | -0.007 | 0.252 | - | - |
| 1.000 | 7 | 0.221 | 0.230 | 0.217 | 6.0 |
| $\phi_2$ 2.253 | 8 | 0.027 | 0.185 | - | - |
| 3.258 | 9 | -0.243 | 0.150 | - | - |
| 6.266 | 10 | -1.666 | 0.043 | - | - |
| 0.407 | 11 | 0.089 | 0.195 | - | - |
| 0.793 | 12 | 0.306 | 0.218 | - | - |
| $\phi_3$ 1.000 | 13 | 0.221 | 0.230 | 0.217 | 6.0 |
| 2.679 | 14 | 0.472 | 0.329 | - | - |
| 6.353 | 15 | 0.513 | 0.547 | - | - |
| 0.414 | 16 | 0.08 | 0.229 | - | - |
| 0.794 | 17 | 0.192 | 0.230 | 0.217 | 6.0 |
| $\phi_4$ 1.000 | 18 | 0.221 | 0.230 | - | - |
| 2.705 | 19 | -0.049 | 0.232 | - | - |
| 6.352 | 20 | 0.373 | 0.236 | - | - |
| Average deviation (%) | | | | | 6.7 |

Table 6 Comparison of flow uniformity index ($\sigma_{out}$) of 3-D turning diffuser obtained from ACFD correlation and experiment

| $\phi_{1,2,3}$ | No. | $\sigma_{out\ 3DTD\ cfd}$ | $\sigma_{out\ 3DTD\ acfd}$ | $\sigma_{out\ 3DTD\ exp}$ | Deviation (%) |
|---|---|---|---|---|---|
| 0.822 | 1 | 2.71 | 3.08 | 2.58 | 19.5 |
| 1.000 | 2 | 2.96 | 3.20 | 3.20 | 0.0 |
| $\phi_1$ 2.590 | 3 | 4.56 | 4.24 | 3.83 | 10.7 |
| 4.792 | 4 | 5.91 | 5.68 | 6.59 | 13.9 |
| 7.735 | 5 | 7.23 | 7.60 | 7.17 | 6.0 |
| 0.381 | 6 | 3.86 | 3.34 | - | - |
| 1.000 | 7 | 2.96 | 3.20 | - | - |
| $\phi_2$ 2.253 | 8 | 2.25 | 2.92 | - | - |
| 3.258 | 9 | 2.51 | 2.70 | - | - |
| 6.266 | 10 | 2.22 | 2.04 | - | - |
| 0.407 | 11 | 3.21 | 3.39 | - | - |
| 0.793 | 12 | 2.52 | 3.27 | - | - |
| $\phi_3$ 1.000 | 13 | 2.96 | 3.20 | 3.20 | 0.0 |
| 2.679 | 14 | 2.04 | 2.67 | - | - |
| 6.353 | 15 | 1.70 | 1.50 | - | - |
| 0.414 | 16 | 3.38 | 3.35 | - | - |
| 0.794 | 17 | 3.02 | 3.25 | - | - |
| $\phi_4$ 1.000 | 18 | 2.96 | 3.20 | 3.20 | 0.0 |
| 2.705 | 19 | 3.3 | 2.77 | - | - |
| 6.352 | 20 | 1.49 | 1.84 | - | - |
| Average deviation (%) | | | | | 7.1 |

## V. CONCLUSION

In conclusion, the current work manages to intensively simulate the effects of geometrical and operating parameters on the performances of 3-D turning diffuser. The performance correlations as a function of geometrical and operating parameters are successfully developed via ACFD with deviation to the experiment approximately of 7%.

## REFERENCES

[1] G. Gan and S.B. Riffat, "Measurement and computational fluid dynamics prediction of diffuser pressure-loss coefficient," *Applied Energy*, vol. 54(2), pp. 181-195, 1996.

[2] W.A. El-Askary and M. Nasr, "Performance of a bend diffuser system: Experimental and numerical studies," *Computer & Fluids*, vol. 38, pp. 160-170, 2009.

[3] R.K. Sullerey, B. Chandra, and V. Muralidhar, "Performance comparison of straight and curved diffusers," *J. of Def. Sci.*, vol. 33, pp. 195-203, 1983.

[4] T.P. Chong, P.F. Joseph and P.O.A.L. Davies, "A parametric study of passive flow control for a short, high area ratio 90 deg curved diffuser," *J. Fluids Eng.*, vol. 130, 2008.

[5] M.K. Gopaliya, M. Kumar, S. Kumar, and S. M. Gopaliya, "Analysis of performance characteristics of S-shaped diffuser with offset," *Aerospace Science & Tech.*, vol. 11, pp. 130-135, 2007.

[6] N. Nordin, V.R. Raghavan, S. Othman and Z.A.A. Karim,"Compatibility of 3-D turning diffusers by means of varying area ratios and outlet-inlet configurations", *ARPN Journal of Engineering and Applied Sciences*, Vol. 7, No. 6, pp 708-713, 2012.

[7] N.Nordin, Z,A.A. Karim, S.Othman and V.R. Raghavan, "The performance of turning diffusers at various inlet conditions". *Applied Mechanics and Materials Journal*, vol. 465-466, pp. 597-602, 2014.

[8] N. Nordin, Z.A.A. Karim, S. Othman, and V. R. Raghavan, "Design & development of low subsonic wind tunnel for turning diffuser application," *Advanced Material Research Journal*, vol. 614-615, pp. 586-591, 2013.

[9] C. Balaji and H. Herwig, "The use of ACFD approach in problems involving surface radiation and free convection", *Int. Comm. Heat and Mass Transfer*, vol. 30, pp 251-259, 2003.
[10] C. Balaji, M. Holling and H.Herwig, "A general methodology for treating mixed convection problems using asymptotic computational fluid dynamics (ACFD)" *Int. Comm. In Heat and Mass Transfer*, vol. 34, pp. 682-691, 2007.
[11] C.Balaji, M.Holling and H.Herwig, "Determination of temperature wall functions for high Rayleigh Number flows using asymptotics: A systematic approach"*Int. Journal of Heat and Mass Transfer*, vol. 50, pp 3820-3831, 2007.
[12] B. Premachandaran and C. Balaji, "Conjugate mixed convection with surface radiation from a horizontal channel with protruding heat sources", Int. Journal of Heat and Mass Transfer, vol. 49, pp 3568-3582, 2006.
[13]N. Nordin, V. R. Raghavan, S. Othman and Z. A. A. Karim, "Numerical investigation of turning diffuser performance by varying geometric and operating parameters", Applied Mechanics and Materials Journal, Vol. 229-231, pp. 2086-2093, 2012.
[14] N.Nordin, Z.A.A. Karim, S.Othman, and V. R. Raghavan," Numerical investigation of turning diffuser performance: Validation and verification," in 2nd Biannual Post Graduate Conference, Tronoh, 2014.
[15] N.Nordin, Z.A.A. Karim, S.Othman, and V. R. Raghavan", Numerical investigation of turning diffuser performance: Validation and verification-Model II", in 3rd Biannual Post Graduate Conference, Tronoh, 2015.

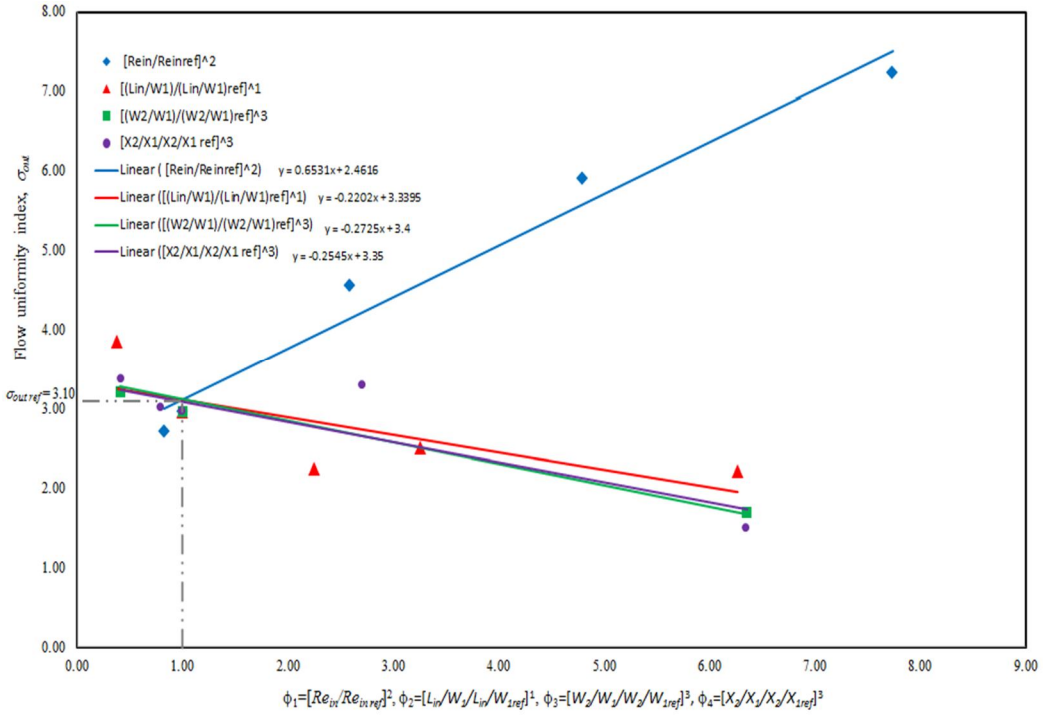


Fig. 11 Flow uniformity index, $\sigma_{out}$ of 3-D turning diffuser with respect to $\phi_1 = [Re_{in}/Re_{in\ ref}]^2$, $\phi_2 = [L_{in}/W_1/L_{in}/W_{1ref}]^1$, $\phi_3 = [W_2/W_1\ /W_2/W_{1ref}]^3$ and $\phi_4 = [X_2/X_1\ /X_2/X_{1ref}]^3$